DØ Note 4741-Conf

Search for the Associated Production of Charginos and Neutralinos in the $e + \tau^{had} + \ell$ Final State

The DØ Collaboration
URL: http://www-d0.fnal.gov
(Dated: March 4, 2005)

A search has been performed for the trilepton decay signature from the associated production of the lightest chargino and the next-to-lightest neutralino. The focus of this search is the $e+\tau+lepton$ final state, where the τ decays hadronically. Data collected from September 2002 through June 2004 by the DØ experiment in Run II of the upgraded Fermilab Tevatron Collider have been used to perform this search. The data corresponds to an integrated luminosity of 325±21 pb^{-1}. No events passing the optimized cuts have been found with the expected background of $0.582^{+0.112}_{-0.105} \pm 0.101$ events.

Preliminary Results for Winter 2005 Conferences

I. INTRODUCTION

The present analysis is based on the MSSM with R-parity conservation ($P_R = (-1)^{3(B-L)+2S}$) [1], which leads to pair production of supersymmetric particles and a stable Lightest Supersymmetric Particle (LSP). The search for associated production of charginos and neutralinos provides the most promising way for the direct detection of supersymmetric partners of weakly interacting particles at the Tevatron. The trilepton channel $\tilde{\chi}^{\pm}\tilde{\chi}^0_2 \rightarrow 3l+\nu\tilde{\chi}^0_1\tilde{\chi}^0_1$ (see Figure 1) is considered the most powerful analysis channel due to its striking signature with three leptons and missing transverse energy ($\not\!\!E_T$), despite the small cross section times branching ratio (typically in the order of 0.5 pb^{-1}) [2]. The topology requiring an electron, a hadronic tau decay and a third isolated track or second tau is considered to be a promising channel for high $\tan\beta$ Supersymmetry (SUSY) scenarios, where the $\tilde{\tau}$ becomes the lightest slepton ($\tilde{\ell}$) due to $\tilde{\tau}$ mixing and therefore enhances the branching ratio into taus. To maintain the highest possible efficiency the third lepton is reconstructed as an isolated track - being efficient for electrons, muons and partly hadronic tau decays - or as a second hadronic tau decay.

Searches for supersymmetric particles have been performed in e^+e^- collisions at LEP [3] and in $p\bar{p}$ collisions at DØ [4] and CDF [5]. Most recent results by DØ in Run II, focusing on the pure leptonic decay of chargino and neutralino, can be found in [6]. No evidence for these particles has been found so far. LSP masses below 40 GeV are excluded in MSSM models with GUT relations by the LEP experiments. In mSUGRA, the LSP lower mass limit is found at 50-60 GeV [3]. For large slepton/sneutrino masses, chargino masses are excluded nearly up to the kinematic production threshold of 103 GeV at LEP [3] by direct searches. Higgs searches at LEP yield indirect sensitivity also for the mass region beyond the chargino production threshold.

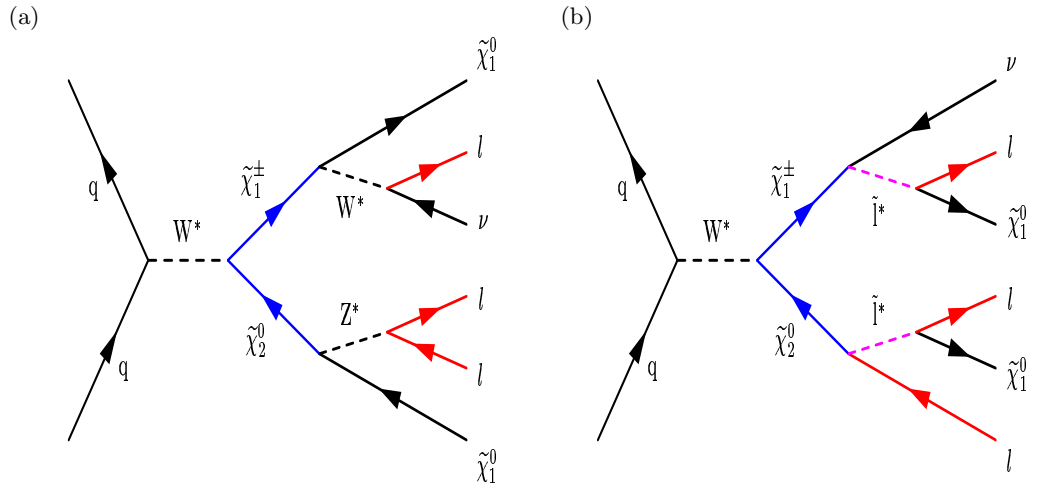

FIG. 1: Feynman diagram for the chargino/neutralino pair production via an off shell W boson in the s-channel and subsequent leptonic decay at leading order via gauge bosons and via sleptons.

II. DATA AND MC SAMPLES

The data sample used in this analysis was collected between August 2002 and June 2004 by the DØ detector at the Fermilab Tevatron $p\bar{p}$ collider at a center-of-mass energy of 1.96 TeV. The corresponding integrated luminosity of this sample is 325.4±21.2 pb^{-1}. All simulated signal and standard model processes are generated using PYTHIA 6.202 [8] and processed through the full detector simulation. Signal parameter combinations have been generated for $\tan\beta = 3$ and chargino masses in the range of 95-130 GeV. The total cross section $\sigma \times \mathrm{BR}(p\bar{p} \rightarrow \tilde{\chi}^{\pm}_1\tilde{\chi}^0_2 \rightarrow 3\ell)$ varies between 0.5 and 0.1 pb. A detailed description of the generated reference points is given in Table I. Higher order QCD corrections (K_{qcd}) have been calculated in [2]. Major background sources include QCD multijet events, $Z/\gamma \rightarrow \tau\tau$, $W \rightarrow e\nu$ and WZ. Multijet background from QCD production is determined directly from data.

TABLE I: Properties of SUSY reference points which were considered in this analysis.

Pt	m_0 [GeV/c^2]	$m_{1/2}$ [GeV/c^2]	A_0 [GeV]	$\tan\beta$	sgn(μ)	# events
C1	64	175	0	3	+	21500
D1	68	180	0	3	+	25500
D4	92	180	0	3	+	21500
E1	72	185	0	3	+	31000

Pt	$m_{\tilde{\chi}_2^0}$ [GeV/c^2]	$m_{\tilde{\chi}^\pm}$ [GeV/c^2]	$m_{\tilde{\chi}_1^0}$ [GeV/c^2]	$m_{\tilde{\ell}}$ [GeV/c^2]	$m_{\tilde{\tau}}$ [GeV/c^2]	$m_{\tilde{\nu}}$ [Gev/c^2]	BR($\tilde{\chi}_2^0$) (e/μ)	(τ)	BR($\tilde{\chi}^\pm$) (e/μ)	(τ)	BR(lep)	$\sigma\times$BR*$K_{\rm qcd}$ [pb]
C1	110	106	60	99	98	122	0.29	0.42	0.04	0.82	0.86	0.692
D1	114	110	62	103	101	128	0.29	0.42	0.04	0.82	0.85	0.579
D4	114	110	62	120	119	142	0.18	0.21	0.15	0.19	0.28	0.180
E1	118	114	65	107	105	133	0.29	0.42	0.04	0.81	0.85	0.489

III. EVENT SELECTION

The event selection starts by requiring an electron candidate matched to a track and a single prong tau candidate. The electron is a calorimeter cluster passing energy isolation, high electromagnetic energy fraction and shower shape cuts and is matched to an isolated reconstructed track. The tau is a narrow calorimeter cluster matched to up to 3 tracks. A set of neural networks (NN) have been developed to make use of discriminating tau variables and to enhance the tau reconstruction efficiency [9]. The tau candidate is either classified as a 1-prong tau with no electromagnetic subcluster(π-like, type 1), as a 1-prong tau with electromagnetic subclusters (ρ-like, type 2) or as 3-prong tau (type 3). Electron and tau object are required to have $\mathrm{p_T} > 8$ GeV and to stem from the same vertex ($|\Delta \mathrm{z_0}| < 2$ cm).

As a cross check for the trilepton analysis in the e+$\tau^{had}+\ell$ final state and to test the tau identification, a comparison of the $\mathrm{Z}/\gamma^* \to \tau\tau \to \mathrm{e} + \tau^{\mathrm{had}}$ signal in data and MC has been performed. The selection strategy is equivalent to the trilepton search, making it an ideal testbed for the latter. The signal was extracted by requiring the neural network output for the tau candidate to be greater than 0.9 ($NN > 0.9$) and an electron. $\mathrm{Z}/\gamma^* \to$ ee background was removed by cutting on the Z mass region, $\Delta\phi$ between the two objects and $E^{\tau}_{had}/{p_T^{\tau}}^{trk}$. Additional cuts on $\not\!\!E_{\mathrm{T}}$ and transverse mass reduce W and QCD backgrounds. The resulting histograms are presented in Figure 2, showing good agreement between data and MC.

Figure 3 shows the invariant $\mathrm{e} + \tau$ mass distribution at the beginning of the SUSY selection. To reduce QCD background from multijet production only 1-prong tau decays (type 1 and 2) with NN > 0.95 are retained (Figure 3). This rejects significantly the background from multijet production where a jet fakes the hadronic tau signature. The $\mathrm{e} + \tau$ sample is further purified by requiring a cut on the electron track isolation. The scalar sum of all tracks within $\Delta\mathrm{R} < 0.4$ of the electron track is required to be smaller than 1 GeV, mostly reducing electron fakes coming from QCD. Requiring the invariant $\mathrm{e} + \tau$ mass to be in the range of $10\,\mathrm{GeV} < \mathrm{M} < 60\,\mathrm{GeV}$ removes mainly $Z \to$ ee. In addition, a part of the back-to-back Drell Yan $\mathrm{Z}/\gamma \to$ ee, the $\mathrm{Z}/\gamma \to \tau\tau$ and the QCD dijet events is rejected by requiring the angle $\Delta\phi$ between the electron and tau candidate to be smaller than 2.9.

Large values of $\not\!\!E_{\mathrm{T}}$ in QCD and Z/γ events can be produced by fluctuations of the reconstructed objects. To reject these events a simple $\not\!\!E_{\mathrm{T}}$ significance is calculated. This quantity, called *scaled* $\not\!\!E_{\mathrm{T}}$ in the following, is calculated in the following way:

$$scaled\ \not\!\!E_{\mathrm{T}} = \frac{\not\!\!E_{\mathrm{T}}}{\sqrt{\sum \left(\sigma(E_T^{jet}) \times |cos(\Delta\phi(jet, \not\!\!E_{\mathrm{T}}))|\right)^2}},\ \text{with}\ \sigma(\mathrm{E_T^{jet}}) = \sqrt{\mathrm{E^{jet}}} \times \sin\theta_{\mathrm{jet}} \tag{1}$$

The scaled $\not\!\!E_{\mathrm{T}}$ is required to be in excess of 8 $\sqrt{\mathrm{GeV}}$.

The scalar sum of the p_T of the jets in the event (H_T) is used to reject $t\bar{t}$ events. A large part can be reduced by requiring $H_T < 60$ GeV, while still keeping a large efficiency for SUSY events.

Poorly measured electron and tau energies often result in large values of the $\not\!\!E_{\mathrm{T}}$ and therefore in small angles to one of the two objects. This leads to small transverse masses of the electron or tau with the missing energy, whereas the signal is characterized by larger transverse masses. Therefore events with a minimum transverse mass ($\mathrm{Min}(\mathrm{MT}(\mathrm{e}, \not\!\!E_{\mathrm{T}}), \mathrm{MT}(\tau, \not\!\!E_{\mathrm{T}}))$) below 10 GeV are discarded (Figure 4).

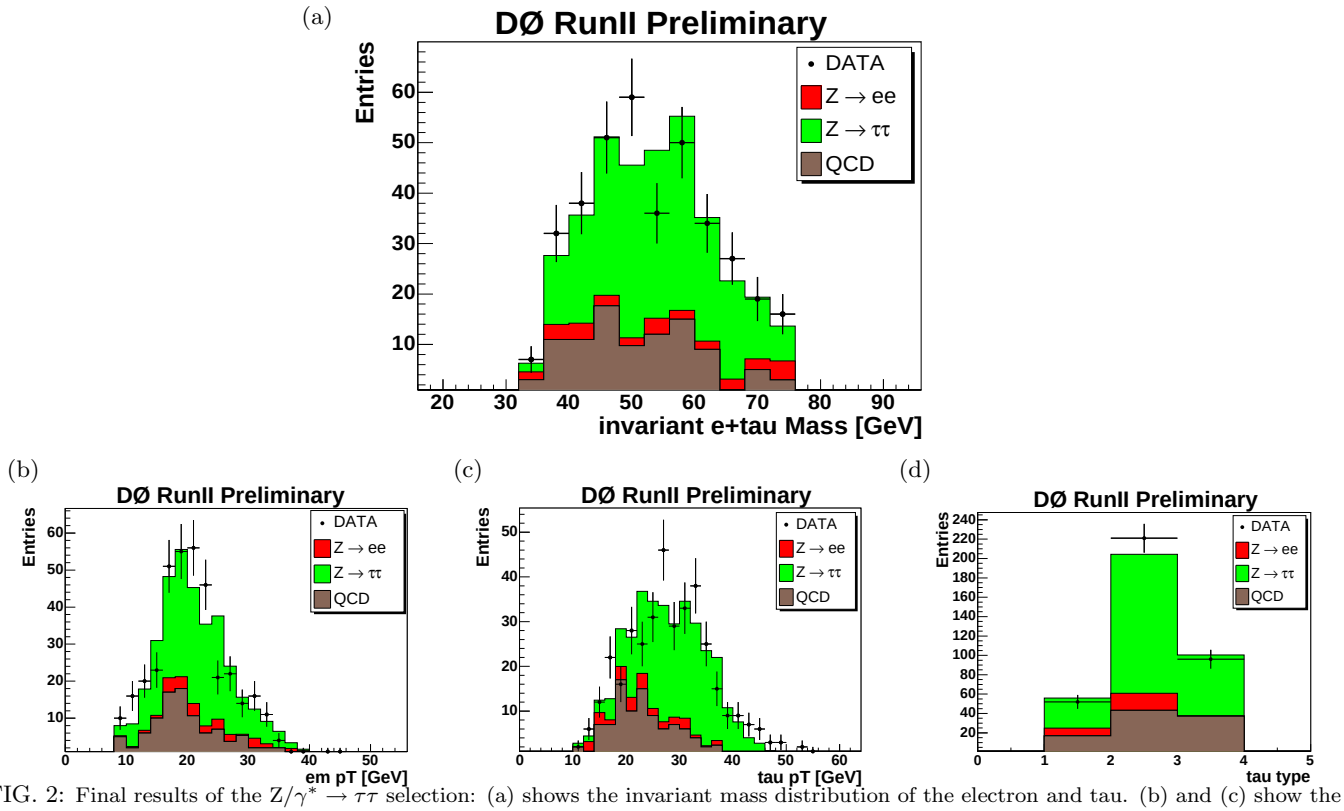

FIG. 2: Final results of the $Z/\gamma^* \to \tau\tau$ selection: (a) shows the invariant mass distribution of the electron and tau. (b) and (c) show the p_T distribution of the electron and tau. (d) shows the tau type distribution (the tau type classification is explained in Section III). Only opposite sign events are shown.

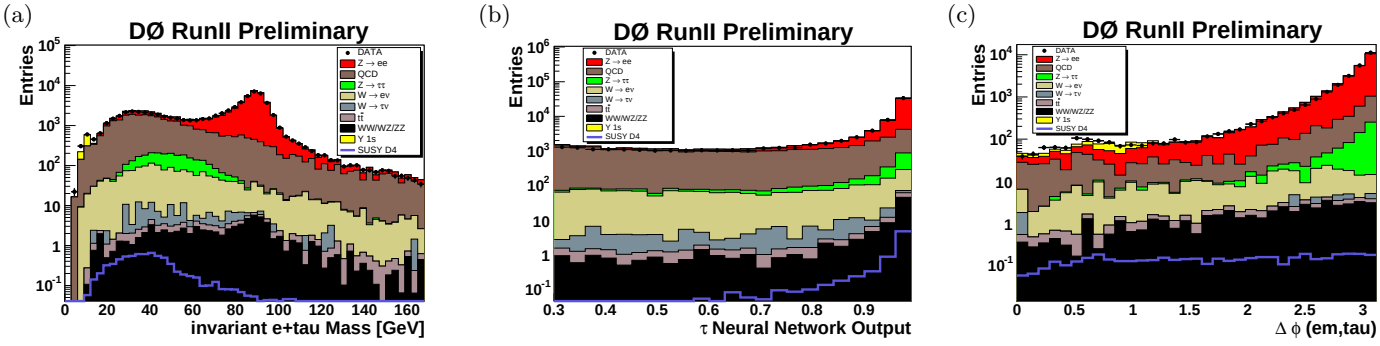

FIG. 3: Distribution of the invariant $e + \tau$ mass (a), the tau neural network output (b) and the $\Delta\phi$-angle between electron and tau (c). Invariant mass and tau neural network output are shown at the beginning of the selection. The $\Delta\phi$ distribution is shown before the Z veto cuts are applied.

$Z/\gamma \to$ ee and QCD di-jet events are characterized by small values of $\not\!\!E_T$, while the two LSPs and the neutrinos in the signal topology lead to a considerable amount of $\not\!\!E_T$. All events with $\not\!\!E_T < 25$ GeV are discarded (Figure 4).

The most important backgrounds remaining after the $\not\!\!E_T$ -cut are QCD and $W \to e\nu$. These backgrounds can be significantly reduced by exploiting the fact that there is a 3rd charged lepton in the SUSY final state. The analysis requires either a second reconstructed tau with NN > 0.95 or an additional isolated track, giving precedence to the second tau (if existing).

The second tau has to be separated by $\Delta R > 0.2$ from both the electron and the first tau. Pick up from $Z \to$ ee, where the second electron is reconstructed as the second tau, is removed by requiring $\Delta\phi < 2.9$ between the leading electron and the second tau. Poorly measured tau energy resulting in large $\not\!\!E_T$ in the direction of the tau is also removed by requiring $\Delta\phi(\not\!\!E_T, \tau_2) > 0.3$. No further cuts are applied to events which have an electron and two taus.

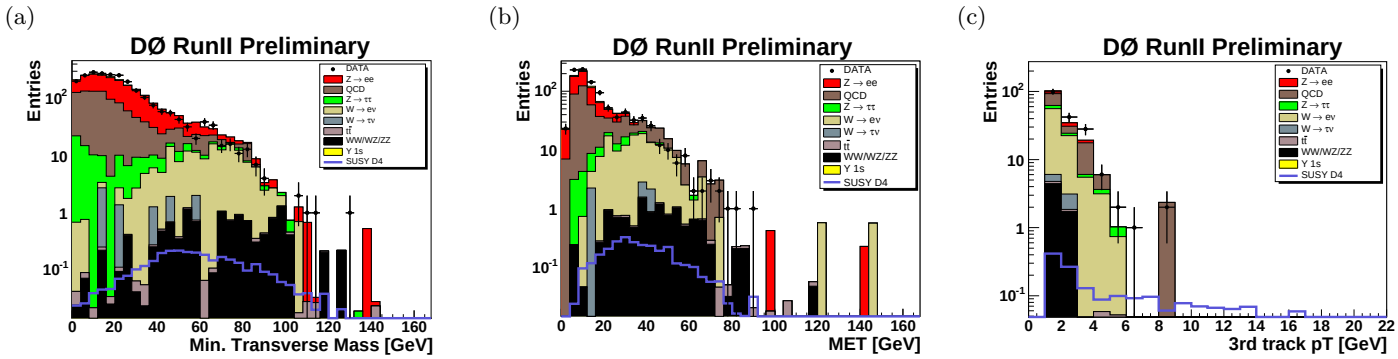

FIG. 4: Distribution of min. transverse mass (a), $\not\!\!E_{\rm T}$ (b) and third track $p_{\rm T}$ (c) before the cut on the variable is applied.

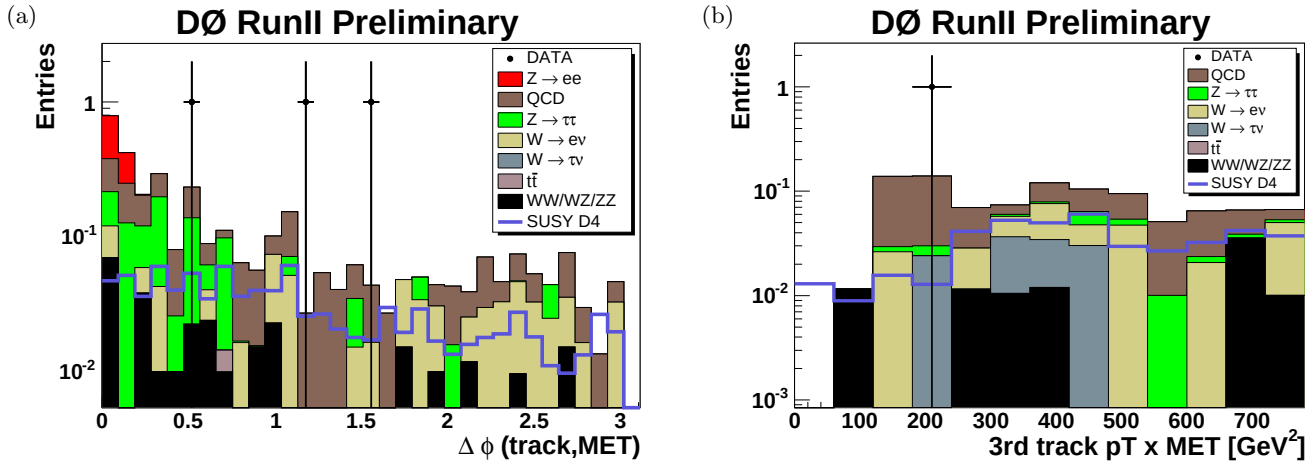

FIG. 5: Distribution of the ϕ-angle between the track and $\not\!\!E_{\rm T}$ (a) and of $p_{\rm T}^{trk}\times \not\!\!E_{\rm T}$ (b) before the cut on the variable is applied.

If no second tau is found in the event an isolated track is required. The track must be well-separated from the electron and tau candidate ($\Delta R > 0.2$), it must come from the same vertex ($|\Delta z_0| < 2\ cm$) and have $p_{\rm T}\ > 5$ GeV (Figure 4). To ensure a good $p_{\rm T}$ measurement, quality cuts on the number of hits in the inner detector are applied. A track isolation is applied requiring the scalar $p_{\rm T}$ sum of all tracks with $0.1 < |\Delta R| < 0.4$ around the track to be $\rm p_T < 1$ GeV. The isolation is designed to be efficient for electrons, muons and hadronic taus.

A further reduction of background events is achieved by cutting on the calorimeter energy deposition in a cone around the third track. The sum of the transverse energy in the electromagnetic and the hadronic cells in a hollow cone of $0.2 < \Delta R < 0.4$ around the track is required to be less than 3 GeV and less than 60% of the $\sqrt{p_{\rm T}(track)}$.

Poorly measured calorimeter energy resulting in large $\not\!\!E_{\rm T}$ in the direction of the track is removed by requiring $\Delta\phi(\not\!\!E_{\rm T}, \rm track) > 0.3$ (Figure 5). The W/Z background can be reduced by cutting on the invariant reconstructed mass of the tau track and the third track ($\rm M(tautrk, trk) < 70$ GeV).

The W background is effectively reduced by raising the $p_{\rm T}$ threshold of the third track to 9 GeV if the transverse mass of the electron and $\not\!\!E_{\rm T}$ is between 50 GeVand 90 GeV, making use of the fact that an additional track in $W \to e\nu$ events has low-$p_{\rm T}$.

The main backgrounds remaining after applying these cuts are coming from QCD, W and W/Z. A further reduction of these background events is achieved by cutting on $p_T^{trk}\times \not\!\!E_{\rm T}$. The final cut value has been determined by varying the cut in the range between 250 GeV^2 and 400 GeV^2 and optimizing the expected limit. All events with $p_T^{trk}\times \not\!\!E_{\rm T} < 350\ GeV^2$ are discarded (Figure 5).

TABLE II: Summary of the applied selection cuts in order to discriminate between signal and background.

(1) Preselection	$p_T^{\rm em} > 8$ GeV, $\rm p_T^{\tau} > 8$GeV same vertex: $\|\Delta z_0\| < 2$ cm tau NN > 0.95
(2) Z veto	$10\,\text{GeV} < \text{inv. mass} < 60\,\text{GeV}$ $\Delta\phi(\text{el}) < 2.9$
(3) Significant MET	$t\bar{t}$ veto: $H_T < 60$ GeV scaled $\not\!\!E_{\rm T} > 8.0\sqrt{\text{GeV}}$ $\text{Min}(\text{MT}(\text{e},\not\!\!E_{\rm T}), \text{MT}(\tau,\not\!\!E_{\rm T})) > 10$ GeV $\not\!\!E_{\rm T} > 25$ GeV
(4) 3rd track OR 2nd tau	track: $p_T > 5$ GeV, track & calorimeter isolation 2nd tau: $p_T > 8$ GeV, NN > 0.95, $\Delta\phi(\tau,\not\!\!E_{\rm T}) > 0.3$
(5) Di-boson veto	$\Delta\phi(\text{trk},\not\!\!E_{\rm T}) > 0.3$ $\text{M}(\text{tau trk}, \text{trk}) < 70$ GeV W veto: $p_T^{\rm trk} > 9$ GeV if 50 GeV $< \text{MT}(\text{e},\not\!\!E_{\rm T}) < 90$ GeV
(6) $p_T^{\rm trk} * \not\!\!E_{\rm T}$	$\not\!\!E_{\rm T} \times p_{\rm T}$ (track) > 350 GeV^2

TABLE III: Number of candidate events observed and background events expected at different stages of the selection for an integrated luminosity of 325.4±21.2 pb^{-1}. The statistical error is listed for all backgrounds.

Cut	Data	Sum BGND	QCD	$Z \to$ee	$Z \to \tau\tau$
(1) Preselection	33466	32572.5±105.9	3092.9±75.7	28289.2±72.7	668.5±6.7
(2) Z veto	2977	2952.4±54.1	1037.9±51.4	1564.8±13.9	136.3±3.9
(3) significant MET	215	220.6±19.0	86.6 ±17.1	15.7±1.7	8.2±0.9
(4) 3rd Track OR 2nd tau	3	$3.271^{+0.800}_{-0.800}$	0.908±0.712	0.588±0.294	0.772±0.188
(5) Di-boson veto	1	$0.977^{+0.225}_{-0.189}$	0.445±0.174	$0.0^{+0.120}_{-0.0}$	0.059±0.017
(6) $p_T^{\rm trk} * \not\!\!E_{\rm T}$	0	$0.582^{+0.112}_{-0.105}$	0.218±0.086	$0.0^{+0.039}_{-0.0}$	0.050±0.015
Cut	$W \to e\nu$	$W \to \tau\nu$	$\Upsilon(1s)$	$WW/WZ/ZZ$	$t\bar{t}$
(1) Preselection	272.7±12.8	8.5±1.9	192.4±4.1	48.6±1.3	16.3±0.3
(2) Z veto	144.6±9.1	7.3±1.7	49.9±2.1	12.7±0.9	5.3±0.2
(3) significant MET	98.5±7.8	2.5±1.0	0.3±0.2	9.6±0.9	0.7±0.1
(4) 3rd Track OR 2nd tau	0.600±0.080	0.103±0.042	$0.0^{+0.009}_{-0.0}$	0.287±0.059	0.013±0.008
(5) Di-boson veto	0.231±0.046	0.103±0.042	$0.0^{+0.002}_{-0.0}$	0.126±0.034	0.013±0.008
(6) $p_T^{\rm trk} * \not\!\!E_{\rm T}$	0.154±0.036	0.031±0.031	$0.0^{+0.002}_{-0.0}$	0.116±0.032	0.013±0.008

IV. RESULTS

The numbers of candidate events observed and background events expected after application of the successive selection cuts are listed in Table III. Selected data and background events are in agreement. No candidate event remains. The background expectation is $0.582^{+0.112}_{-0.105} \pm 0.101$ events, mostly stemming from QCD, $W \to e\nu$ and WZ events. The error on the background expectation is dominated by the limited statistics. The numbers of events expected for the chosen SUSY samples are shown in Table IV.

Various sources of systematic uncertainties have been studied to investigate their influence on signal efficiencies and

TABLE IV: Number of signal events expected at different stages of the selection with statistical error.

Cut	C1	D1	D4	E1
$m_{\tilde{\chi}^{\pm}}$(GeV)	106	110	110	114
(1) Preselection	11.20±0.29	9.58±0.21	4.67±0.09	8.73±0.17
(2) Z veto	9.23±0.25	7.57±0.18	3.59±0.08	6.90±0.15
(3) Significant MET	5.90±0.20	4.80±0.15	2.38±0.07	4.46±0.12
(4) 3rd Track OR 2nd tau	1.986±0.115	1.747±0.111	0.973±0.044	1.382±0.069
(5) Di-boson veto	1.271±0.093	1.271±0.093	0.691±0.037	1.059±0.059
(6) $p_T^{\rm trk} * \not\!\!E_{\rm T}$	1.116±0.087	1.116±0.087	0.634±0.035	0.968±0.057

background expectations. A large contribution for both signal and background comes from the 6.5 % error on the integrated luminosity. Further systematic uncertainties for the background are related to the jet calibration (15.4 %) and the QCD estimate (7 %). MC corrections for the trigger turn-on and the track efficiency contribute with 2.5 % resp. 2.8 %. The calibration of electrons and $\not\!\!E_{\rm T}$ contributes with 1.5 % and 1.6 %. This results in a total systematic error for the background estimate of 17.3% in the final selection. The systematic error on the signal expectation adds up to 7.4 %, mostly stemming from the track efficiency (2.8 %), the trigger turn-on (1.8 %) and $\not\!\!E_{\rm T}$ smearing (1.1 %).

V. CONCLUSIONS

A search has been performed for the trilepton decay signature from the associated production of the lightest chargino and the next-to-lightest neutralino in leptonic channels, focusing on the $e + \tau + lepton$ final state where the τ decays hadronically. The analysis is not yet sensitive for mSUGRA points which were considered, but the sensitivity can be increased in combination with the $\mathrm{e} + \mathrm{e} + l$, $\mathrm{e} + \mu + l$, $\mu + \mu + l$, LS $\mu + \mu$ and $\mu + \tau^{had} + l$ analyses.

Acknowledgments

We thank the staffs at Fermilab and collaborating institutions, and acknowledge support from the Department of Energy and National Science Foundation (USA), Commissariat à l'Energie Atomique and CNRS/Institut National de Physique Nucléaire et de Physique des Particules (France), Ministry of Education and Science, Agency for Atomic Energy and RF President Grants Program (Russia), CAPES, CNPq, FAPERJ, FAPESP and FUNDUNESP (Brazil), Departments of Atomic Energy and Science and Technology (India), Colciencias (Colombia), CONACyT (Mexico), KRF (Korea), CONICET and UBACyT (Argentina), The Foundation for Fundamental Research on Matter (The Netherlands), PPARC (United Kingdom), Ministry of Education (Czech Republic), Canada Research Chairs Program, CFI, Natural Sciences and Engineering Research Council and WestGrid Project (Canada), BMBF and DFG (Germany), Science Foundation Ireland, A.P. Sloan Foundation, Research Corporation, Texas Advanced Research Program, Alexander von Humboldt Foundation, and the Marie Curie Fellowships.

[1] H.P. Nilles, Phys. Rep. **110** (1984) 1;
H.E. Haber and G.L. Kane, Phys. Rep. **117** (1985) 75,
[2] W.Beenakker *et al.,* "*The production of Charginos/Neutralinos and Sleptons at Hadron Colliders* ", hep-ph/9906298,
[3] LEPSUSYWG, ALEPH, DELPHI, L3 and OPAL experiments,
note LEPSUSYWG/01-07.1, (`http://lepsusy.web.cern.ch/lepsusy /Welcome.html`),
[4] B.Abbott *et al.,* Phys. Rev. Lett. **80** (1998) 8,
[5] F. Abe *et al.,* "*Search for Chargino-Neutralino Associated Production at the Fermilab Tevatron Collider* ", Phys. Rev. Lett. **80**, 5275 (1998)
[6] The DØ Collaboration `http://www-d0.fnal.gov/Run2Physics/WWW/results/prelim/NP/N11/N11.pdf`,
[7] DØ Collaboration, V. Abazov *et al.*, "The Upgraded DØ Detector", in preparation for submission to Nucl. Instrum. Methods Phys. Res. A, and T. LeCompte and H.T. Diehl, Ann. Rev. Nucl. Part. Sci **50**, 71 (200)
[8] T. Sjostrand, Comp. Phys. Commun. **82** (1994) 74, `CERN-TH 7112/93` (1993),
[9] The DØ Collaboration, "*First measurement of* $\sigma(\mathrm{p\bar{p}} \rightarrow Z) \times BR(Z \rightarrow \tau\tau)$ *at a center-of-mass energy of 1.96 TeV* ", FERMILAB-PUB-04/381-E